

DESY-98-154  
OUTP-98-68-P

# Non-perturbative quark mass renormalization in quenched lattice QCD



Stefano Capitani<sup>a</sup>, Martin Lüscher<sup>a</sup>, Rainer Sommer<sup>b</sup> and Hartmut Wittig<sup>c,1</sup>

<sup>a</sup> Deutsches Elektronen-Synchrotron, DESY  
Notkestrasse 85, D-22603 Hamburg, Germany

<sup>b</sup> DESY-Zeuthen  
Platanenallee 6, D-15738 Zeuthen, Germany

<sup>c</sup> Theoretical Physics, University of Oxford  
1 Keble Road, Oxford OX1 3NP, UK

## Abstract

The renormalization factor relating the bare to the renormalization group invariant quark masses is accurately calculated in quenched lattice QCD using a recursive finite-size technique. The result is presented in the form of a product of a universal factor times another factor, which depends on the details of the lattice theory but is easy to compute, since it does not involve any large scale differences. As a byproduct the  $\Lambda$ -parameter of the theory is obtained with a total error of 8%.

October 1998

---

<sup>1</sup>PPARC Advanced Fellow

## 1 Introduction

The masses of the light quarks are not directly accessible to experiment and have to be determined through a non-perturbative calculation, taking low-energy hadronic data (such as the kaon masses) as input. Chiral perturbation theory is able to predict their ratios with a precision of a few percent [1]. In order to obtain estimates of individual quark masses, it thus suffices to determine a particular linear combination using lattice QCD [2–13] or QCD sum rules [14–23].

Calculations of quark masses in lattice QCD are in principle straightforward, but there are several sources of systematic errors which must be studied carefully (for recent reviews of the subject see [24, 25]). One of the principal uncertainties arises from the renormalization constant needed to convert from lattice normalizations to the  $\overline{\text{MS}}$  scheme of dimensional regularization. Usually this factor is only known in one-loop perturbation theory in the bare coupling. The limitations of lattice perturbation theory are well known, and in order to remove all doubts about the reliability of quark mass calculations in lattice QCD, it is evident that a non-perturbative determination of the renormalization factor is required.

The general problem of non-perturbative renormalization of QCD addresses the question how the perturbative regime of QCD is related to the observed hadrons and their interactions. This relation involves large scale differences, and thus the problem is not easily approached using numerical simulations, for which only a limited range of lattice spacings is accessible.

A strategy how to overcome this technical difficulty has been described in [26], and a comprehensive introduction into the subject is presented in [27]. An alternative method was introduced in [28] and is actively being pursued [4, 12, 29, 30]. In our strategy the key idea is the introduction of an intermediate renormalization scheme, with a controlled (non-perturbative) relation to the lattice normalizations, and in which the scale evolution of masses and couplings can be computed non-perturbatively from low to very high energies. In the high-energy regime one can continue the scale evolution using perturbation theory, which allows for the determination of the renormalization group invariant quark masses  $M$  and the  $\Lambda$ -parameter. Since the matching of  $M$  and  $\Lambda$  between different renormalization schemes is exactly computable, it is evident that all reference to the intermediate scheme is eliminated at this stage.

Thus, the problem of non-perturbative quark mass renormalization can be split into two parts. The first is the computation of the scale dependence of the running masses  $\overline{m}$  in the intermediate scheme from low to high energies and its relation to the renormalization group invariant quark masses  $M$ . The ratio  $\overline{m}/M$  is then known at all energy scales covered by the calculation. The second part is the matching of the renormalized masses  $\overline{m}$  with the bare current quark masses  $m(g_0)$ . This amounts to the computation of  $\overline{m}/m(g_0)$  at a certain value of the energy scale which is chosen as the matching point. Since the matching can be performed at low energies, no excessively large lattices are required to contain all relevant scales. Whereas the second part clearly

depends on the details of the lattice regularization, such as the chosen lattice action and the bare coupling, the ratio  $\bar{m}/M$  is a universal quantity.

In this work we have calculated the regularization independent factor  $\bar{m}/M$  in quenched QCD, using the Schrödinger functional (SF) as our intermediate renormalization scheme. We emphasize that the SF scheme is chosen entirely for practical purposes, since it allows the non-perturbative computation of the scale dependence over several orders of magnitude in a controlled way, using a recursive finite-size scaling technique and numerical simulations. The numerical results for the scale dependence of  $\bar{m}$  can be extrapolated reliably to the continuum limit, so that a truly universal result for  $\bar{m}/M$  is obtained.

In addition, we have computed the matching between the renormalized quark masses in the SF scheme and the bare quark masses in  $O(a)$  improved lattice QCD [31] for a range of bare couplings at a fixed scale. Thus, by combining the universal ratio  $\bar{m}/M$  with the matching factor  $\bar{m}/m(g_0)$  we have obtained the total renormalization factor  $M/m(g_0)$ , which relates the bare current quark masses to the renormalization group invariant quark masses.

We also report on our determination of the  $\Lambda$ -parameter in quenched QCD. For this purpose, we have supplemented the numerical data for the running coupling published in [32], so that the scale evolution could be traced over more than two orders of magnitude. Preliminary results of our calculations have been presented in [33].

The rest of the paper is organized as follows. In Sect. 2 we discuss the scale dependence of the running coupling and quark masses in perturbation theory. The Schrödinger functional scheme is described in detail in Sect. 3. The step scaling functions, which describe the scale evolution of the running parameters, are briefly discussed in Sect. 4. In Sect. 5 we describe the extraction of  $\bar{m}/M$  and the  $\Lambda$ -parameter. The matching of these results to hadronic schemes is presented in Sect. 6, and Sect. 7 contains our conclusions. In order to avoid distracting the reader from the main results, we defer all technical details about the computation of the step scaling functions, the error propagation in the scale evolution and the calculation of  $\bar{m}/m(g_0)$  to Appendices A, B and C, respectively.

## 2 Running coupling and quark masses in perturbation theory

### 2.1 Mass-independent renormalization schemes

QCD is a theory with  $N_f + 1$  free parameters: its coupling constant  $g$  and the masses of the  $N_f$  different quark flavours,  $\{m_s, s = 1, \dots, N_f\}$ . In the definition of the theory through a regularization, these are initially taken to be the bare parameters in the Lagrangian. Upon removal of the regularization, one defines renormalized parameters,  $\bar{g}$ ,  $\{\bar{m}_s, s = 1, \dots, N_f\}$  at some energy scale  $\mu$ . In the following we assume that the normalization conditions which are imposed to define  $\bar{g}$ ,  $\bar{m}_s$  are independent of the quark masses themselves. Examples for such mass-independent renormalization schemes are the  $\overline{\text{MS}}$  scheme of dimensional regularization [34, 35] and the Schrödinger functional

(SF) scheme [26, 36]. The latter will be described in Sect. 3. The renormalized running parameters are then functions of the renormalization scale  $\mu$  alone, and their scale evolution is given by the renormalization group equations

$$\mu \frac{\partial \bar{g}}{\partial \mu} = \beta(\bar{g}), \quad (2.1)$$

$$\mu \frac{\partial \bar{m}_s}{\partial \mu} = \tau(\bar{g}) \bar{m}_s, \quad s = 1, \dots, N_f. \quad (2.2)$$

The renormalization group functions,  $\beta$  and  $\tau$ , have a perturbative expansion

$$\beta(\bar{g}) \stackrel{\bar{g} \rightarrow 0}{\sim} -\bar{g}^3 \left\{ b_0 + b_1 \bar{g}^2 + b_2 \bar{g}^4 + \dots \right\}, \quad (2.3)$$

$$\tau(\bar{g}) \stackrel{\bar{g} \rightarrow 0}{\sim} -\bar{g}^2 \left\{ d_0 + d_1 \bar{g}^2 + d_2 \bar{g}^4 + \dots \right\}. \quad (2.4)$$

The universal coefficients  $b_0$ ,  $b_1$  and  $d_0$  are given by

$$b_0 = (4\pi)^{-2} \left\{ 11 - \frac{2}{3} N_f \right\}, \quad b_1 = (4\pi)^{-4} \left\{ 102 - \frac{38}{3} N_f \right\}, \quad (2.5)$$

$$d_0 = 8/(4\pi)^2, \quad (2.6)$$

whereas the higher order coefficients  $b_2, b_3, \dots$  and  $d_1, d_2, \dots$  depend on the chosen renormalization scheme. Equations (2.1, 2.2) can be solved straightforwardly. This yields the exact relations between the scale dependent quantities  $\bar{g}(\mu), \bar{m}_s(\mu)$  and the renormalization group invariants,

$$\Lambda = \mu (b_0 \bar{g}^2)^{-b_1/2b_0^2} e^{-1/2b_0 \bar{g}^2} \times \exp \left\{ - \int_0^{\bar{g}} dg \left[ \frac{1}{\beta(g)} + \frac{1}{b_0 g^3} - \frac{b_1}{b_0^2 g} \right] \right\}, \quad (2.7)$$

$$M_s = \bar{m}_s (2b_0 \bar{g}^2)^{-d_0/2b_0} \times \exp \left\{ - \int_0^{\bar{g}} dg \left[ \frac{\tau(g)}{\beta(g)} - \frac{d_0}{b_0 g} \right] \right\}. \quad (2.8)$$

Unlike the case of the  $\Lambda$ -parameter, there is no universally accepted normalization convention for the renormalization group invariant quark masses  $M_s$ . Eq. (2.8) complies with the conventions used by Gasser and Leutwyler [37].

In contrast to  $\bar{g}$  and  $\bar{m}_s$ , the renormalization group invariants  $\Lambda$  and  $M_s$  do not depend on the scale; from a technical point of view they are the integration constants of the differential equations (2.1, 2.2). From eq. (2.8) and the scale independence of  $M_s$ , we read off immediately that ratios of running quark masses,  $\bar{m}_s/\bar{m}_{s'}$ , are scale independent in mass-independent renormalization schemes, and are equal to  $M_s/M_{s'}$ .

The renormalization group invariant quark masses are easily shown to be independent of the renormalization scheme, while the  $\Lambda$ -parameter changes from scheme to scheme by factors that can be calculated exactly. It is hence natural to take  $\Lambda$  and the renormalization group invariant quark masses  $M_s$  as the fundamental parameters of QCD.

Furthermore one concludes that in order to extract the fundamental parameters of QCD, one may choose a scheme which is particularly suited for the computation of  $\Lambda$  and  $M_s$ .

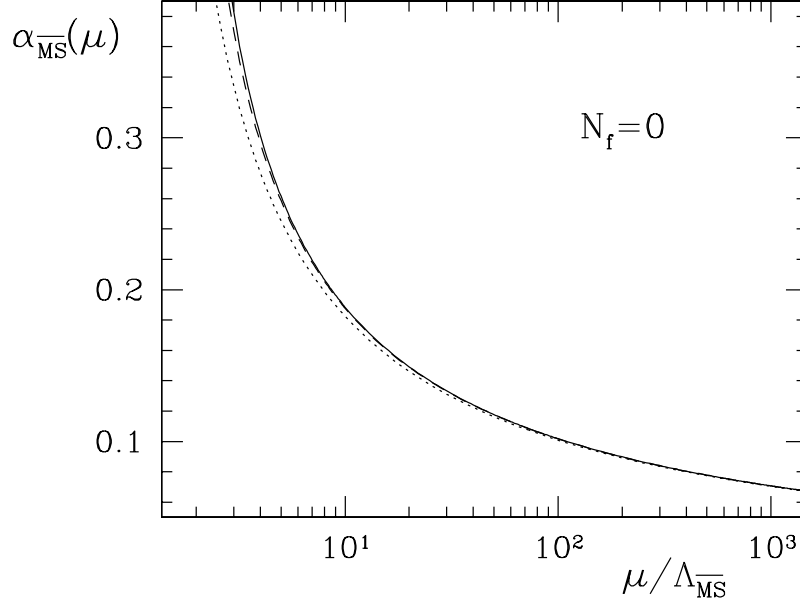


**Figure 1:** Running coupling  $\alpha_{\overline{\text{MS}}} = \bar{g}_{\overline{\text{MS}}}^2/4\pi$  in quenched QCD. From the dotted to the full curve, the perturbative accuracy increases from two to four loops.

## 2.2 Illustration: the $\overline{\text{MS}}$ scheme

In the  $\overline{\text{MS}}$  scheme the perturbative expansions eqs. (2.3,2.4) are known to four loops [38–48]. Here we use them to plot the evolution of the running coupling and quark masses in this scheme for  $N_f = 0$  flavours. The dotted, dashed and full curves in Figs. 1 and 2 have been obtained from eqs. (2.7) and (2.8) by substituting the 2-, 3- and 4-loop expressions for the  $\beta$ - and  $\tau$ -functions and computing the integrals in the exponents numerically.

Conventionally the running coupling and quark masses are quoted in the  $\overline{\text{MS}}$  scheme at a certain value of the normalization mass  $\mu$ . Figures 1 and 2 illustrate that, once  $\Lambda$  and  $M$  are known, the running parameters in the  $\overline{\text{MS}}$  scheme are uniquely determined to any given order of perturbation theory.

As we shall see in Sect. 6 the value of  $\Lambda_{\overline{\text{MS}}}$  in quenched QCD is about 240 MeV. From Figs. 1 and 2 one infers that perturbation theory appears to “converge” at energies as low as 1 GeV. However, since the  $\overline{\text{MS}}$  scheme is only defined to any finite order of perturbation theory, it is impossible to make a solid statement about the total uncertainty in the running coupling and quark masses at a certain reference scale. In other words, the running coupling and quark masses in the  $\overline{\text{MS}}$  scheme are only meaningful to a given order of perturbation theory.

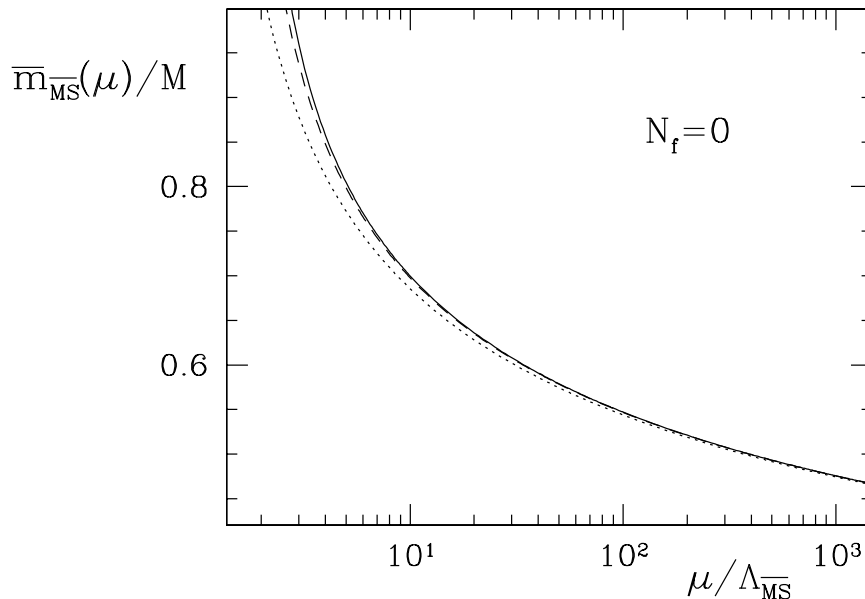


**Figure 2:** Running quark mass in quenched QCD. The flavour index has been omitted, since the entire graph is independent of which quark flavour is considered.

### 3 The Schrödinger functional scheme

In this section we describe the intermediate renormalization scheme, which we have used to relate hadronic observables to the renormalization group invariant parameters. The chosen scheme, defined using the Schrödinger functional, has been the subject of a series of publications [32, 36, 49–52]. For clarity we repeat the basic concepts of the Schrödinger functional but shall otherwise be rather brief and refer the reader to the literature for details. A pedagogical introduction can be found in [27].

#### 3.1 General definitions

As already mentioned in the introduction, the main difficulty of relating the observed hadron spectrum to the perturbative regime of QCD in a controlled way is the large scale difference. Non-perturbative renormalization such as the approach introduced in [28] relies on all relevant physical scales being accommodated on a single lattice. This results in a rather narrow energy range which can be explored.

It has been demonstrated [53] that this problem can be overcome by simulating a sequence of lattices with decreasing lattice spacing. Any single lattice only covers a limited range of distances, but through the use of a finite-volume renormalization scheme it is possible to match subsequent lattices. With only a few steps of this procedure one can easily cover a much larger energy range than otherwise possible.

The Schrödinger functional is a particular finite-volume renormalization scheme. It is based on the formulation of QCD in a finite space-time volume of size  $T \times L^3$ , with periodic spatial boundary conditions and inhomogeneous Dirichlet boundary conditions at time  $x_0 = 0$  and  $x_0 = T$  [49, 50]. This is realized by requiring the spatial components of the gauge field at the boundary to be equal to some prescribed constant abelian fields  $C$  and  $C'$ . This choice of boundary condition introduces a frequency gap on the quark and gluon fields, so that simulations for vanishing quark mass can be performed.

We take over the exact form of the action and the boundary conditions from Sect. 2.1 of ref. [52]; any notation not explained here is taken over from that reference. The definition of the scheme requires that the ratio  $T/L$  is kept fixed. For reasons that will be explained below we have set  $T = L$  throughout this work. Within this set-up, renormalization conditions are then specified at scale  $\mu = 1/L$  and vanishing quark mass. Thus, the Schrödinger functional is a mass-independent renormalization scheme, in which the running coupling and masses scale with the box size  $L$ .

### 3.2 Running coupling and masses

Our next task is to specify exactly the definition of the running coupling and quark masses in the SF scheme, which we have used in the numerical simulations. In particular, we will exploit the freedom in choosing the boundary fields  $C$  and  $C'$ , and the angle  $\theta$  which appears in the spatial boundary conditions of quark fields. From a practical point of view, these have to be chosen with care in order to ensure that the scale evolution of masses and couplings can be determined with high accuracy in the continuum limit and that contact with the perturbative evolution at high energies can easily be made.

The “optimal” definitions of  $\bar{g}$  and  $\bar{m}$  [32, 36, 49, 52] are obtained by considering the following criteria:

- Choose observables with small variance in Monte Carlo simulations to ensure good statistical precision of the results;
- Avoid parameter values which introduce “accidentally” large coefficients in the perturbative expansion of e.g. the  $\beta$ - and  $\tau$ -functions;
- Minimize the contamination of coupling and quark mass by lattice artefacts.

The renormalized coupling at length scale  $L$  is given in terms of an infinitesimal variation of the boundary conditions for the gauge fields, exactly as defined in refs. [32, 52], where all details can be found. It is denoted by  $\bar{g}(L)$ , whereas in accordance with standard notation in the  $\overline{\text{MS}}$  scheme, we choose the corresponding energy scale as argument for  $\alpha$ , viz.

$$\alpha(\mu) = \frac{\bar{g}^2(L)}{4\pi}, \quad \mu = 1/L. \quad (3.1)$$

We now describe the definition of the running quark mass  $\overline{m}(\mu)$  in more detail and introduce it formally in the framework of continuum QCD. Its definition is easily made rigorous in the lattice regularization (see Appendix A.2 and [36]). The starting point is the PCAC relation,

$$\partial_\mu (A_R)_\mu = (\overline{m}_s + \overline{m}_{s'}) P_R, \quad (3.2)$$

between the renormalized axial current,

$$(A_R)_\mu(x) = Z_A \overline{\psi}_s(x) \gamma_\mu \gamma_5 \psi_{s'}(x), \quad (3.3)$$

and the pseudoscalar density,

$$P_R(x) = Z_P \overline{\psi}_s(x) \gamma_5 \psi_{s'}(x). \quad (3.4)$$

Once eq. (3.2) is chosen to define the quark masses, their normalization is given in terms of the normalization of  $A_R$  and  $P_R$ . The axial current is normalized naturally through current algebra relations [54–62] and does not acquire a scale dependence through renormalization. Therefore, both scheme- and scale-dependence are contained in the definition of  $P_R$ .

In order to formulate a normalization condition for the pseudoscalar density, we set [36],

$$T = L, \quad C = C' = 0, \quad \theta = 1/2. \quad (3.5)$$

This choice is motivated by the criteria listed above, and a more detailed explanation is given in ref. [36]. We then start from the correlation functions

$$f_P(x_0) = -\frac{1}{3} \int d^3\mathbf{y} d^3\mathbf{z} \langle \overline{\psi}(x) \gamma_5 \frac{1}{2} \tau^a \psi(x) \bar{\zeta}(\mathbf{y}) \gamma_5 \frac{1}{2} \tau^a \zeta(\mathbf{z}) \rangle \quad (3.6)$$

$$f_1 = -\frac{1}{3L^6} \int d^3\mathbf{u} d^3\mathbf{v} d^3\mathbf{y} d^3\mathbf{z} \langle \bar{\zeta}'(\mathbf{u}) \gamma_5 \frac{1}{2} \tau^a \zeta'(\mathbf{v}) \bar{\zeta}(\mathbf{y}) \gamma_5 \frac{1}{2} \tau^a \zeta(\mathbf{z}) \rangle, \quad (3.7)$$

involving the boundary quark fields,  $\zeta, \dots, \bar{\zeta}'$  [63]. Here and in the following, the Pauli-matrices,  $\tau^a$ , are understood to act on the first two flavour components of the quark fields. As the renormalization is flavour-blind in a mass-independent renormalization scheme, this is sufficient to define the renormalization constants. Furthermore we introduce bare current quark masses  $m_s$  via

$$\partial_\mu [\overline{\psi}_s(x) \gamma_\mu \gamma_5 \psi_{s'}(x)] = (m_s + m_{s'}) \overline{\psi}_s(x) \gamma_5 \psi_{s'}(x), \quad (3.8)$$

and define the renormalization constant

$$Z_P(L) = \frac{\sqrt{3f_1}}{f_P(L/2)}, \quad \text{at } m_s = 0, \quad s = 1, \dots, N_f. \quad (3.9)$$



Here, the numerator  $\sqrt{f_1}$  is introduced to cancel the multiplicative renormalization of the boundary quark fields  $\zeta$  and  $\bar{\zeta}$ , which appear in the definition of  $f_P$ . Our convention eq. (3.9) ensures that  $Z_P = 1$  at tree level of perturbation theory.

Explicitly the definition of the running quark masses in the SF scheme now reads

$$\bar{m}(\mu)_s = \frac{Z_A}{Z_P(L)} m_s, \quad \mu = 1/L. \quad (3.10)$$

The above expressions are easily given a precise meaning in the lattice regularization, and we refer to the formulae listed in Appendix A.2.1. We emphasize, however, that the SF-scheme is not linked to a particular regularization. Note that  $Z_P$  is defined in terms of correlation functions at finite physical distances for which on-shell  $O(a)$  improvement may be applied [63, 64] to reduce lattice artefacts. Although this detail is irrelevant for the definition of the scheme itself, it will be important in its numerical implementation.

From now on we will drop the flavour index  $s$  on all quark masses, except when we refer to a particular flavour.

Finally we note that the normalization constant  $Z_A$  of the axial current is known non-perturbatively in  $O(a)$  improved quenched lattice QCD [62]. Hence, in order to determine the complete renormalization factor in eq. (3.10), it suffices to compute the renormalization constant  $Z_P$ .

### 3.3 Perturbation theory

The SF scheme has been studied perturbatively in quite some detail. In the rest of this section we list the results which are relevant for the present computation, setting  $N_f = 0$ . All quantities where we do not indicate the scheme explicitly refer to the SF scheme. The  $\Lambda$ -parameter is translated to the  $\overline{\text{MS}}$  scheme via [32]

$$\Lambda = 0.48811(1)\Lambda_{\overline{\text{MS}}}, \quad (3.11)$$

and the three-loop coefficient of the  $\beta$ -function was determined as [65]

$$b_2 = 0.483(9)/(4\pi)^3. \quad (3.12)$$

In addition, the two-loop anomalous dimension of the quark mass,

$$d_1 = 0.217(1)/(4\pi)^2, \quad (3.13)$$

was computed as part of this project [36]. Given the perturbative expansion coefficients of  $\beta$  and  $\tau$  in the  $\overline{\text{MS}}$  scheme, these equations fix the one-loop relation of  $\bar{m}$  to  $\bar{m}_{\overline{\text{MS}}}$  and the two-loop relation of  $\alpha$  to  $\alpha_{\overline{\text{MS}}}$ . Explicit formulae may be found in [36, 65].

For our purposes, the coefficients  $b_2$  and  $d_1$  serve primarily to continue the scale evolution of the running coupling and quark mass in the SF scheme to infinite energy using perturbation theory. This allows for the extraction of  $\Lambda$  and  $M$ , which can be easily converted into their counterparts in the  $\overline{\text{MS}}$  scheme through eq. (3.11) and the fact that  $M = M_{\overline{\text{MS}}}$ .

$u$	$\sigma(u)$	$\sigma_P(u)$
0.8873	0.981(9)	0.9683(21)
0.9944	1.110(11)	0.9672(23)
1.0989	1.252(11)	0.9622(24)
1.2430	1.416(16)	0.9579(29)
1.3293	1.528(20)	0.9470(28)
1.4300	1.703(24)	0.9407(30)
1.5553	1.865(23)	0.9382(33)
1.6950	2.095(25)	0.9297(32)
1.8811	2.412(32)	0.9284(36)
2.1000	2.771(41)	0.9168(37)
2.4484	3.464(40)	0.8942(38)
2.7700		0.8781(42)
3.4800		0.8451(55)

**Table 1:** Simulation results for the step scaling functions  $\sigma(u)$  and  $\sigma_P(u)$

## 4 Step scaling functions

In the SF scheme a change of the renormalization scale amounts to a change of the box size  $L$  at fixed bare parameters. By considering a sequence of pairs of volumes with sizes  $L$  and  $2L$ , one can thus study the evolution of the running coupling and quark masses under repeated changes of the scale by a factor 2. Effectively one constructs a non-perturbative renormalization group in this way.

The evolution from size  $L$  to  $2L$  of the running coupling and the normalization of the pseudoscalar density is described by the step scaling functions  $\sigma(u)$  and  $\sigma_P(u)$  according to

$$\bar{g}^2(2L) = \sigma(u), \quad u \equiv \bar{g}^2(L), \quad (4.1)$$

$$Z_P(2L) = \sigma_P(u) Z_P(L). \quad (4.2)$$

For a given lattice resolution  $a/L$  both functions can be computed non-perturbatively through numerical simulations of the Schrödinger functional. It is important to realize that the box size  $L$  can be as small as we like in these calculations. The only restriction is that  $L$  and the low-energy physical scales in the theory should be significantly larger than the lattice spacing to avoid uncontrolled cutoff effects.

The step scaling function associated with the coupling has first been computed in ref. [32]. We have extended these calculations so that  $\sigma(u)$  is now known precisely for altogether 11 values of  $u$  (see Table 1). Moreover we have obtained  $\sigma_P(u)$  at the same couplings and, in addition, at  $u = 2.77$  and  $u = 3.48$ . The technical details of our computations are summarized in Appendix A. Here we only mention that the

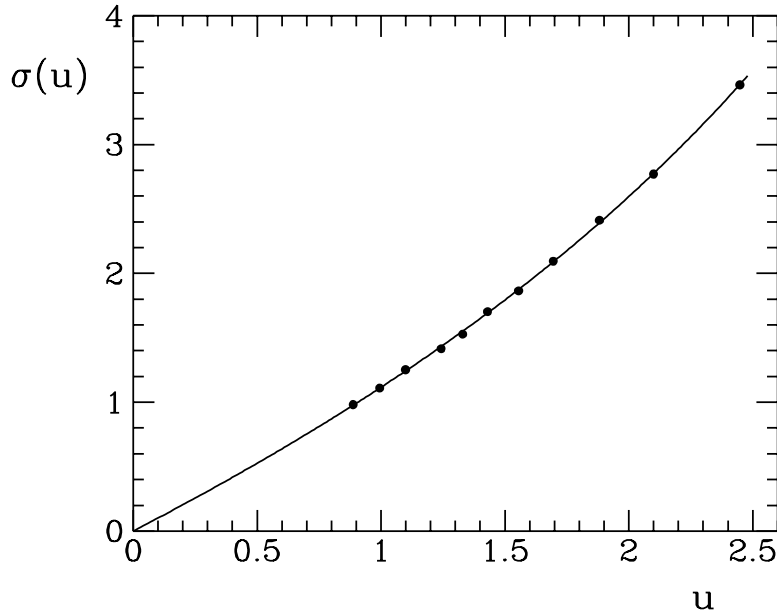


**Figure 3:** Polynomial fit of the data for the step scaling function  $\sigma(u)$ . The errors on the data are about equal to the symbol size.

lattice results for the step scaling functions depend on the lattice spacing and have to be extrapolated to the continuum limit. The extrapolation is required but not critical, since in all cases considered the observed lattice effects are small, particularly after including the relevant  $O(a)$  correction terms.

## 5 Running coupling and quark mass in the SF scheme

Having computed the step scaling functions, we can now work out the evolution of the coupling and the quark masses over roughly two decades of the energy scale. It should be stressed from the beginning that all results obtained in this section refer to the continuum theory. The basic idea is to start from some initial values at low energies and to step up the energy scale by factors of 2 by repeated application of the step scaling functions. In terms of the box size  $L$  this leads us from some large size  $L_{\max}$  to smaller sizes  $2^{-k}L_{\max}$ . Eventually the perturbative regime is reached and perturbation theory may then be used to extract the  $\Lambda$ -parameter and the renormalization group invariant quark masses.

The largest value of  $\bar{g}^2$  which can be reached with the available data for the step scaling function  $\sigma(u)$  is 3.48. We thus define the scale  $L_{\max}$  through

$$\bar{g}^2(L) = 3.48 \quad \text{at} \quad L = L_{\max}. \quad (5.1)$$

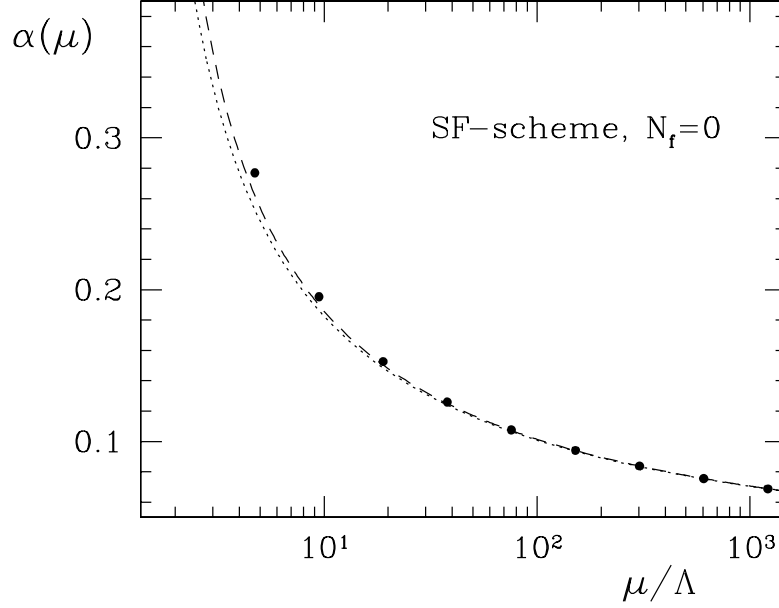


**Figure 4:** Comparison of the numerically computed values of the running coupling in the SF scheme with perturbation theory. The dotted and dashed curves are obtained from eq. (2.7) using the 2- and 3-loop expressions for the  $\beta$ -function. The errors on the data are smaller than the symbol size.

The sequence of couplings<sup>2</sup>

$$u_k = \bar{g}^2(2^{-k}L_{\max}), \quad k = 0, 1, 2, \dots, \quad (5.2)$$

can then be calculated by solving the recursion

$$u_0 = 3.48, \quad \sigma(u_{k+1}) = u_k. \quad (5.3)$$

A technical problem here is that  $\sigma(u)$  is only known at certain values of the coupling and only to a finite numerical precision. This difficulty can be resolved by fitting the data with a polynomial, as shown in Fig. 3, and using the fit function in the recursion (5.3). The analysis presented in Appendix B shows that the systematic uncertainty which is incurred by this procedure is negligible compared to the statistical errors, provided one stays in the range of couplings covered by the data.

After six steps the recursion yields

$$\bar{g}^2(L) = 1.053(12) \quad \text{at} \quad L = 2^{-6}L_{\max} \quad (5.4)$$

and two more iterations bring us down to a value of 0.865(11). As will become clear below, these couplings are deep in the high-energy regime where the scale evolution is

---

<sup>2</sup>Note that, contrary to the convention used in [33], the box size  $L$  decreases for increasing  $k$ .

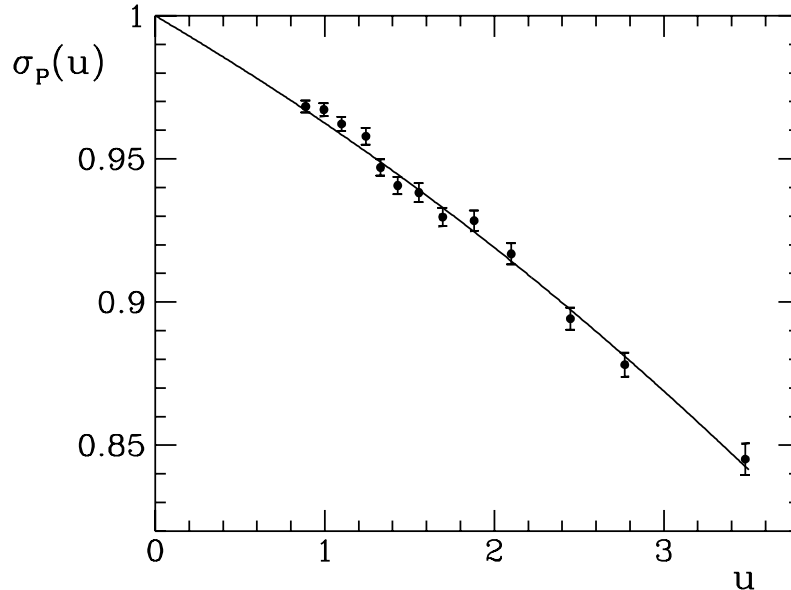


**Figure 5:** Polynomial fit of the data for the step scaling function  $\sigma_P(u)$ .

accurately described by perturbation theory. The  $\Lambda$ -parameter may thus be calculated by setting  $\mu = 1/L$  in eq. (2.7) and inserting the coupling quoted above. To evaluate the integral in this formula, one may safely use the 3-loop expression for the  $\beta$ -function since the coupling is small in the whole integration range (if an approximately geometric progression of the coefficients  $b_k$  is assumed, the error from the neglected higher-order terms is an order of magnitude smaller than the statistical error). As result one obtains

$$\Lambda = 0.211(16)/L_{\max} \quad (5.5)$$

and from Fig. 4 one can now see that the numerically determined values of the coupling are indeed closely matched by the perturbative evolution in the range where the  $\Lambda$ -parameter has been extracted. In this plot the error in eq. (5.5) has not been taken into account since it amounts to an overall scale shift which is of no relevance for the comparison of the scale evolution of the coupling with perturbation theory.

We now proceed to discuss the scale dependence of the renormalized pseudoscalar density and the running quark mass. In this case the data for the step scaling functions listed in Table 1 allow us to trace the scale evolution up to  $L = 2L_{\max}$ . If we define

$$v_k = Z_P(2^{-k+1}L_{\max})/Z_P(2L_{\max}), \quad k = 0, 1, 2, \dots, \quad (5.6)$$

the recursion to be solved is

$$v_0 = 1, \quad v_{k+1} = v_k/\sigma_P(u_k), \quad (5.7)$$

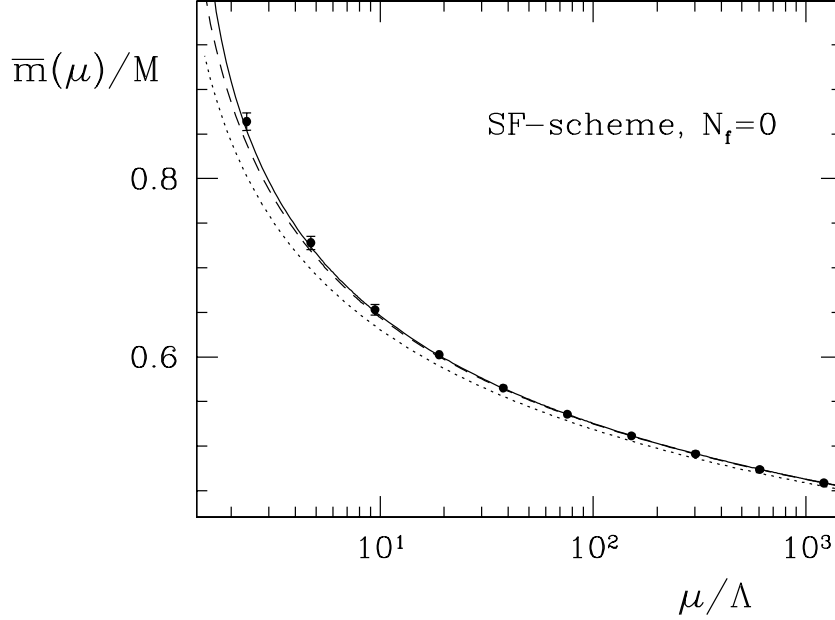


**Figure 6:** Comparison of the numerically computed values of the running quark mass in the SF scheme with perturbation theory. The dotted, dashed and solid curves are obtained from eqs. (2.7) and (2.8) using the 1/2-, 2/2- and 2/3-loop expressions for the  $\tau$ - and  $\beta$ -functions respectively.

where  $u_k$ ,  $k \geq 0$ , is the sequence of couplings introduced above. Using the fit for  $\sigma_P(u)$  displayed in Fig. 5 it is straightforward to perform this calculation and after seven steps one finds

$$Z_P(L)/Z_P(2L_{\max}) = 1.759(15) \quad \text{at} \quad L = 2^{-6}L_{\max} \quad (5.8)$$

(see Appendix B for further details). At this point the coupling is so small that it is safe to insert the two- and three-loop expressions for the  $\tau$ - and  $\beta$ -function in eq. (2.8). Taking eq. (5.8) into account the result

$$M/\bar{m}(\mu) = 1.157(12) \quad \text{at} \quad \mu = (2L_{\max})^{-1} \quad (5.9)$$

is then obtained. Similar to the coupling, the scale evolution of the running quark masses in the SF scheme is accurately reproduced by perturbation theory down to surprisingly low energies (see Fig. 6).

## 6 Matching to hadronic observables

At this point the  $\Lambda$ -parameter and the renormalization group invariant quark masses  $M$  are known in terms of the reference scale  $L_{\max}$  and the running quark masses  $\bar{m}(\mu)$  at  $\mu = (2L_{\max})^{-1}$ . To complete the calculation we now need to relate  $L_{\max}$  and  $\bar{m}(\mu)$  to a hadronic scheme, where the parameters of the theory are fixed by requiring a set

of low-energy hadronic quantities to assume their physical values. It should again be emphasized that this step does not involve any large scale differences. In particular, the calculations can be carried out using lattices which cover all relevant scales, as in a conventional hadron mass computation.

### 6.1 Computation of $\Lambda_{\overline{\text{MS}}}$

We now describe how to convert the result for the  $\Lambda$ -parameter in eq. (5.5) into  $\Lambda_{\overline{\text{MS}}}$  expressed in terms of a hadronic scale. A convenient hadronic reference scale is the radius  $r_0$  which has been introduced in ref. [66]. It is defined through the force between static quarks and is thus a purely gluonic quantity in the quenched approximation, similarly to  $\bar{g}^2(L)$  and  $L_{\text{max}}$ . Relating  $L_{\text{max}}$  to  $r_0$  is straightforward, but requires data for  $r_0/a$  with good precision for a range of  $g_0$ , in order to obtain the continuum limit [67]. As part of our project, the ratio  $L_{\text{max}}/r_0$  was computed [67],

$$L_{\text{max}}/r_0 = 0.718(16). \quad (6.1)$$

We can now remove all reference to the intermediate renormalization scheme and quote the  $\Lambda$ -parameter in units of  $r_0$ . By combining eqs. (6.1), (5.5) and (3.11) we obtain

$$\Lambda_{\overline{\text{MS}}}^{(0)} = 0.602(48)/r_0, \quad (6.2)$$

where the superscript  $^{(0)}$  reminds us that this quantity has been determined for  $N_f = 0$ , i.e. in the quenched theory. For illustration, physical units can be introduced by setting  $r_0 = 0.5 \text{ fm}$ , which gives <sup>3</sup>

$$\Lambda_{\overline{\text{MS}}}^{(0)} = 238(19) \text{ MeV}. \quad (6.3)$$

However, as is well known, the conversion to physical units is ambiguous in the quenched approximation. The solid result is eq. (6.2).

### 6.2 Computation of the total renormalization factor

Next we describe the calculation of the renormalization factor  $Z_M(g_0)$  which relates the bare current quark masses  $m$  to the renormalization group invariant quark masses  $M$ . The renormalized current quark masses have been defined in eq. (3.8), and their definition in the  $O(a)$  improved lattice theory is given in eq. (A.7). By including the appropriate renormalization factors for the axial current and the pseudoscalar density we can now write down the relation between  $M$  and  $m$  in  $O(a)$  improved lattice QCD, viz.

$$M = \frac{M}{\bar{m}(\mu)} \frac{Z_A(g_0)(1 + b_A a m_q)}{Z_P(g_0, L)(1 + b_P a m_q)} m + O(a^2), \quad \mu = 1/L. \quad (6.4)$$

---

<sup>3</sup>The value of  $\Lambda_{\overline{\text{MS}}}^{(0)}$  differs from the result quoted in [27, 33], because  $L_{\text{max}}/r_0$  has been recalculated in ref. [67].

Here, the subtracted mass  $m_q$  is defined by  $m_q = m_c - m_0$ , where  $m_c$  is the critical value of the bare quark mass  $m_0$  (c.f. ref. [63]).

The improvement coefficients  $b_A$  and  $b_P$  are defined in [63]. A strategy how to compute them non-perturbatively has been described recently in [68], but no results for our choice of action have been reported so far. However, the difference  $b_A - b_P$ , which is relevant in the above relation has been shown to be small [69, 70]. Therefore it appears safe to neglect  $b_A$  and  $b_P$  altogether, provided that one is interested in the light quark masses only.

After these considerations we define

$$Z_M(g_0) = \frac{M}{\bar{m}(\mu)} \frac{Z_A(g_0)}{Z_P(g_0, L)}, \quad \mu = 1/L, \quad (6.5)$$

such that

$$M = Z_M(g_0) m(g_0) + O(a^2). \quad (6.6)$$

Thus the total renormalization  $Z_M$  consists of the regularization independent part  $M/\bar{m}$  and the ratio  $Z_A/Z_P$ , which depends on the details of the lattice formulation. In eq. (6.5) all reference to the SF scheme has disappeared, so that  $Z_M$  depends only on the lattice regularization. Furthermore  $Z_M$ , contrary to  $Z_P$ , is independent of the matching point.

As described in Sect. 5 the ratio  $M/\bar{m}$  is obtained for scales  $\mu$  down to a minimum value of  $\mu = (2L_{\max})^{-1}$ . It is therefore natural to choose

$$L = 1.436 r_0 \quad (6.7)$$

as the value of the matching scale, which is twice the central value of  $L_{\max}$  in eq. (6.1). We obtain

$$M/\bar{m}(\mu) = 1.157(15) \quad \text{at} \quad \mu = (1.436 r_0)^{-1}. \quad (6.8)$$

The error in eq. (6.8) contains a small contribution from the error in eq. (6.1), which was estimated using the perturbative scale dependence of  $\bar{m}$ .

The next step in the determination of  $Z_M$  is the calculation of  $Z_A(g_0)/Z_P(g_0, L)$  at the matching point  $L = 1.436 r_0$  for a range of bare couplings. Results for the normalization constant of the axial current,  $Z_A$ , have been presented in [62]. Eq. (6.11) in ref. [62] describes  $Z_A(g_0)$  with an accuracy of 1 % for  $g_0 \leq 1$ .

We have now also computed  $Z_P$  in the range  $6.0 \leq \beta \leq 6.5$ ,  $\beta = 6/g_0^2$ . The details of the calculation are explained in Appendix C, and results listed in Table 8 and in eq. (C.3). They are represented by a polynomial fit

$$Z_P(g_0, L/a)_{L=1.436 r_0} = 0.5233 - 0.0362(\beta - 6) + 0.0430(\beta - 6)^2, \\ \beta = 6/g_0^2, \quad 6.0 \leq \beta \leq 6.5, \quad (6.9)$$

which is shown together with the data for  $Z_P$  in Fig. 7. The formula describes the data with a statistical uncertainty of about 0.5%.



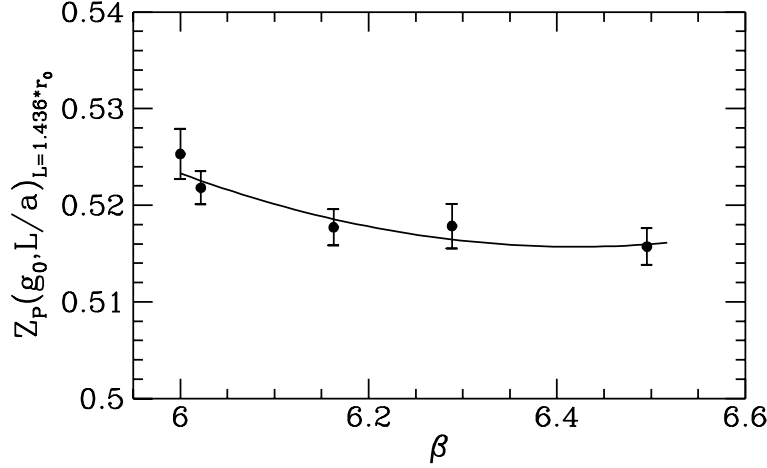


**Figure 7:** Numerical results for  $Z_P(g_0, L/a)_{L=1.436 r_0}$ . The solid line represents the fit eq. (6.9).

$\beta$	$Z_P$	$Z_A$	$Z_M$
6.0	0.5233(26)	0.7906(94)	1.748(23)(23)
6.2	0.5178(26)	0.8067(76)	1.803(19)(23)
6.4	0.5157(26)	0.8273(78)	1.856(20)(24)

**Table 2:** Results for  $Z_P$ ,  $Z_A$  and  $Z_M$  at typical values of  $\beta = 6/g_0^2$

By combining the results for  $M/\bar{m}$ ,  $Z_A$  and  $Z_P$ , we can now compute  $Z_M$ . Results at commonly used values of  $\beta$  are listed in Table 2. The entries for  $Z_P$  and  $Z_A$  in the table have been taken from the parametrization eq. (6.9) and Table 2 of ref. [62], respectively. The first error quoted for  $Z_M$  comes from the uncertainty in the ratio  $Z_A/Z_P$ , whereas the second arises from the error in  $M/\bar{m}$  at the matching scale. It is useful to separate the two sources of error, since  $M/\bar{m}$  has been computed in the continuum limit. Therefore, it does not make sense to include the error quoted in eq. (6.8) in the continuum extrapolation of lattice data for current quark masses. Instead the uncertainty of 1.3% in  $M/\bar{m}(\mu)$  at  $\mu = (1.436 r_0)^{-1}$  should be added in quadrature to the quark mass *after* the extrapolation has been performed.

As in the case of  $Z_P$ , it is convenient to represent the results for  $Z_M$  in terms of a polynomial fit function. For bare couplings in the range  $6.0 \leq \beta \leq 6.5$  the data for  $Z_M(g_0)$  are well described by the expression

$$Z_M(g_0) = 1.752 + 0.321 (\beta - 6) - 0.220 (\beta - 6)^2. \quad (6.10)$$

This parametrization yields  $Z_M$  with an accuracy of about 1.1%, if the error in  $M/\bar{m}$  is

neglected.

As explained in detail in Appendix C the results for  $Z_P$  are subject to a systematic error of order  $a$ , due to imperfect knowledge of the improvement coefficient  $c_t$ . Our estimates of this systematic error show that it is negligible in most applications. In fact, the error in the total renormalization  $Z_M$  is clearly dominated by the uncertainty in  $Z_A$ , but not by residual  $O(a)$  effects in  $Z_P$ .

We now discuss briefly the application of our results for  $Z_M$ . Let us assume that we want to compute the sum of up and strange quark masses,  $M_u + M_s$ . Using lattice data for the hadronic scale  $r_0$  [67] and the bare current quark masses computed in the  $O(a)$  improved theory one can compute the dimensionless quantity

$$Z_M(g_0) \times (m_u + m_s)(g_0) \times r_0(g_0). \quad (6.11)$$

Depending on the chosen values of the bare coupling,  $Z_M$  can be taken either from Table 2 (using the first of the two quoted errors) or the parametrization in eq. (6.10) (with an uncertainty of 1.1%). An extrapolation in  $(a/r_0)^2$  to the continuum limit yields the value of  $M_u + M_s$  in units of  $r_0$ . At this point the error of 1.3% in  $M/\bar{m}$  at the matching scale should be added in quadrature to the result. Estimates for the light quark masses using our values of  $Z_M$  will be published elsewhere [71].

### 6.3 $Z_M$ for different lattice actions

The results for  $Z_M$  presented here have been obtained in  $O(a)$  improved lattice QCD using the action defined in [31]. If a different discretization of the QCD action were chosen,  $Z_M$  would have to be recomputed. It is now important to realize that the calculation of the universal part of  $Z_M$ , i.e. the ratio  $M/\bar{m}$  does not have to be repeated, since it is independent of the regularization. This represents a considerable saving of CPU time, since the most difficult and demanding part in the determination of  $Z_M$  is the calculation of the scale dependence of  $M/\bar{m}$  from low to very high energies. Therefore, only the calculation of  $Z_A$  (as outlined in [62]) and  $Z_P$  has to be performed for a different lattice action.

## 7 Conclusions

In this paper we have demonstrated that the relation between the fundamental parameters of QCD and hadronic observables can be computed non-perturbatively with controlled errors. Our main results have been obtained in the quenched approximation, but our methods carry over literally to full QCD. That is, no additional conceptual difficulties are expected, as long as one is interested in QCD with up, down and strange quarks only.

By combining a recursive finite-size technique with lattice simulations we have calculated the scale evolution of quark masses in the Schrödinger functional renormalization scheme, starting from energies of a few hundred MeV up to scales well above

100 GeV, where contact with perturbative scaling could be made. In this way we were able to extract the ratio  $M/\overline{m}$  at  $\mu = (1.436 r_0)^{-1}$ . Similarly, by computing the scale evolution of the running coupling we calculated the  $\Lambda$ -parameter without compromising approximations. By means of a careful removal of lattice artefacts in the computation of the scale evolution we have obtained universal results for  $M/\overline{m}$  and the  $\Lambda$ -parameter.

Another main result of our work is the calculation of the renormalization factor of the pseudoscalar density in  $O(a)$  improved lattice QCD for a range of bare couplings. We have computed this factor in the SF scheme at the lowest energy matching point. The results can be combined with the previously computed renormalization factor of the axial current [62] and the universal factor  $M/\overline{m}$ . Thereby we have determined the total renormalization factor which relates the bare quark masses in the  $O(a)$  improved lattice theory to the renormalization group invariant quark masses.

Our results for  $\Lambda_{\overline{\text{MS}}}^{(0)}$  and the relation between the bare current quark masses and  $M$  are not subject to systematic errors other than the use of the quenched approximation. In this sense our method to compute renormalization factors of scale-dependent quantities is rather unique. Another advantage is that renormalization factors can be computed for vanishing quark mass. The method is generally applicable to the problem of scale-dependent renormalization and is now also being used to compute renormalization constants for low moments of structure functions [72].

Usually quark masses are quoted in the  $\overline{\text{MS}}$  scheme at normalization mass  $\mu = 1 \text{ GeV}$  or  $\mu = 2 \text{ GeV}$ . Once a non-perturbative solution of the theory becomes possible, this convention is not entirely satisfactory, because the  $\overline{\text{MS}}$  scheme is only meaningful to any finite order of perturbation theory. On the other hand, the renormalization group invariant quark masses are non-perturbatively defined and scheme-independent. Hence, they are more quotable than the  $\overline{\text{MS}}$  masses, and we would like to recommend their use in future studies.

This work is part of the ALPHA collaboration research programme. We are grateful to Roberto Petronzio for computer time on the APE/Quadrics at the University of Rome “Tor Vergata”, and to Giulia de Divitiis and Tereza Mendes for their help.

## A Computation of step scaling functions on the lattice

### A.1 Calculation of $\sigma(u)$

The calculation starts from the lattice step scaling function  $\Sigma(u, a/L)$  defined as in the continuum but for finite resolution  $a/L$ . Its precise definition was given in ref. [32]. We followed closely this reference. In particular we took exactly the same discretization and set the improvement coefficient  $c_t$  to its value in one-loop perturbation theory [32],

$$c_t^{1\text{-loop}} = 1 - 0.089g_0^2. \quad (\text{A.1})$$

One then has to be aware that lattice spacing errors linear in the lattice spacing are not suppressed completely, because perturbation theory approximates  $c_t$  with unknown precision.

Apart from numerical checks and a few simulations on the smallest systems, the simulations were performed on APE-100 parallel computers with 128 to 512 nodes. We employed the hybrid overrelaxation algorithm described in Sect. 3.1 of [31], setting  $N_{\text{OR}} = L/(2a)$ . For renormalized couplings of around  $u = 3.5$ , we used the modified sampling introduced in Appendix A of [32] with parameter  $\gamma = 0.02 - 0.05$ .

Numerical results for running couplings on pairs of lattices  $L/a, 2L/a$  at the respective values of  $\beta = 6/g_0^2$ , are listed in Table 3 for future reference. The data have been analyzed as in ref. [32], by propagating the error of  $\bar{g}^2(L)$  into  $\Sigma(u, a/L)$ , where  $u$  is the central value of  $\bar{g}^2(L)$ . We then extrapolated  $\Sigma(u, a/L)$  to the continuum limit, allowing for the expected dominant discretization error linear in  $a/L$ . In practice we fit

$$\Sigma(u, a/L) = \sigma(u) + \omega(u) a/L. \quad (\text{A.2})$$

These fits have good  $\chi^2$ . We list the fit parameters  $\sigma(u)$ , the slopes  $\omega(u)$  and the  $\chi^2$  together with the number of degrees of freedom in the fit,  $n_{\text{df}}$ , in Table 4. One observes that at the level of our precision lattice artefacts are not significant. Alternatively one could assume that  $c_t$  is well approximated by its one-loop perturbative estimate in eq. (A.1), so that  $a/L$  effects are negligible. An extrapolation using a quadratic ansatz,  $(a/L)^2$ , for the leading lattice artefacts would give entirely consistent values for  $\sigma(u)$  but smaller statistical errors.

In Table 1 we have included the results for  $\sigma(u)$  from Table 4 and those in Table 4 of ref. [32].

$\beta$	$L/a$	$\bar{g}^2(L)$	$\bar{g}^2(2L)$	$\Sigma(u, a/L)$
10.6064	5	0.8873(5)	0.9736(28)	0.9736(29)
10.7503	6	0.8873(5)	0.9712(29)	0.9712(30)
10.8790	7	0.8873(5)	0.9767(31)	0.9767(32)
11.0000	8	0.8873(10)	0.9759(28)	0.9759(31)
9.9024	5	0.9944(6)	1.1070(32)	1.1070(33)
10.0500	6	0.9944(7)	1.1044(38)	1.1044(39)
10.1835	7	0.9944(7)	1.1024(38)	1.1024(39)
10.3000	8	0.9944(13)	1.1127(41)	1.1127(44)
9.3518	5	1.0989(7)	1.2318(41)	1.2318(42)
9.5030	6	1.0989(8)	1.2350(46)	1.2350(47)
9.6272	7	1.0989(8)	1.2434(35)	1.2434(36)
9.7500	8	1.0989(13)	1.2364(34)	1.2364(38)
8.4582	5	1.3293(10)	1.5541(62)	1.5541(63)
8.6129	6	1.3293(12)	1.5409(52)	1.5409(54)
8.7431	7	1.3293(11)	1.5442(76)	1.5442(77)
8.8500	8	1.3293(21)	1.5461(70)	1.5461(76)
7.8583	5	1.5553(13)	1.8776(93)	1.8776(95)
7.9993	6	1.5553(15)	1.8811(38)	1.8813(43)
8.1380	7	1.5553(19)	1.884(11)	1.884(12)
8.2500	8	1.5553(24)	1.864(10)	1.864(11)
8.5873	12	1.5553(50)	1.879(17)	1.879(19)
7.2611	5	1.8811(19)	2.388(15)	2.388(15)
7.4082	6	1.8811(22)	2.397(17)	2.397(18)
7.5438	7	1.8811(26)	2.374(18)	2.374(18)
7.6547	8	1.8811(28)	2.393(18)	2.393(18)
7.9993	12	1.8811(38)	2.411(20)	2.411(21)
6.6255	5	2.4484(32)	3.504(16)	3.504(17)
6.7807	6	2.4484(37)	3.478(22)	3.478(23)
6.9079	7	2.4484(56)	3.501(17)	3.501(21)
7.0197	8	2.4484(45)	3.484(21)	3.484(23)
6.9748	9	2.4484(58)	3.496(42)	3.496(44)
7.3551	12	2.4484(80)	3.475(26)	3.475(31)

**Table 3:** Pairs of renormalized couplings and the step scaling function  $\Sigma$

$u$	$\sigma(u)$	$\omega(u)$	$\chi^2/n_{\text{df}}$
0.8873	0.981(9)	-0.04(5)	1.3/2
0.9944	1.110(11)	-0.02(7)	3.3/2
1.0989	1.252(11)	-0.10(7)	3.0/2
1.3293	1.528(20)	0.11(12)	1.7/2
1.5553	1.865(23)	0.09(14)	2.4/4
1.8811	2.412(32)	-0.14(21)	1.5/3
2.4484	3.464(40)	0.19(25)	0.9/4

**Table 4:** Continuum extrapolation of the step scaling function  $\Sigma$  according to eq. (A.2)

## A.2 Calculation of $\sigma_P(u)$

We now describe the details of the numerical calculations which we have performed to determine the step scaling function for  $Z_P$ . This involves the calculation of correlation functions constructed in the framework of the Schrödinger functional in a lattice simulation. Here we have used the  $O(a)$  improved Wilson action defined in [63]. We take over the notation introduced in that reference.

### A.2.1 Definitions

As explained in Sect. 3, the renormalization constant  $Z_P$  is defined in terms of correlation functions involving the pseudoscalar density and the boundary quark fields. On the lattice these correlation functions are represented by

$$f_P(x_0) = -a^6 \sum_{\mathbf{y}, \mathbf{z}} \frac{1}{3} \langle \bar{\psi}(x) \gamma_5 \frac{1}{2} \tau^a \psi(x) \bar{\zeta}(\mathbf{y}) \gamma_5 \frac{1}{2} \tau^a \zeta(\mathbf{z}) \rangle, \quad (\text{A.3})$$

$$f_1 = -\frac{a^{12}}{L^6} \sum_{\mathbf{u}, \mathbf{v}, \mathbf{y}, \mathbf{x}} \frac{1}{3} \langle \bar{\zeta}'(\mathbf{u}) \gamma_5 \frac{1}{2} \tau^a \zeta'(\mathbf{v}) \bar{\zeta}(\mathbf{y}) \gamma_5 \frac{1}{2} \tau^a \zeta(\mathbf{z}) \rangle. \quad (\text{A.4})$$

They have been formally defined in the continuum theory in eqs. (3.6,3.7), and we use the same symbols to denote the lattice correlation functions.

The normalization constant  $Z_P$  of the pseudoscalar density is then defined by

$$Z_P(g_0, L/a) = c \frac{\sqrt{3f_1}}{f_P(L/2)} \quad (\text{A.5})$$

at vanishing quark mass. The constant  $c$  is chosen so that  $Z_P = 1$  at tree level. For  $\theta = 1/2$ , which is chosen in our simulations, we list values for  $c$  in Table 5. They differ from unity by small terms of order  $(a/L)^2$ .

We now need to specify the precise definition of the quark mass used in the determination of  $Z_P$  and the step scaling function. The reason is that the point of vanishing

current quark mass is not unambiguously defined in a regularization without exact chiral symmetry. For instance, in the  $O(a)$  improved theory there is an uncertainty of order  $a^2$ . The details of the definition will influence the size of  $O(a^2)$  lattice artefacts in the lattice step scaling function, but not its continuum limit. Following ref. [31] we introduce the correlation function of the (unimproved) bare axial current

$$f_A(x_0) = -a^6 \sum_{\mathbf{y}, \mathbf{z}} \frac{1}{3} \langle \bar{\psi}(x) \gamma_0 \gamma_5 \frac{1}{2} \tau^a \psi(x) \bar{\zeta}(\mathbf{y}) \gamma_5 \frac{1}{2} \tau^a \zeta(\mathbf{z}) \rangle, \quad (\text{A.6})$$

and define an unrenormalized current quark mass  $m(g_0)$  through

$$m(g_0) = \frac{\frac{1}{2}(\partial_0^* + \partial_0) f_A(x_0) + c_A a \partial_0^* \partial_0 f_P(x_0)}{2f_P(x_0)}. \quad (\text{A.7})$$

Here,  $\partial_0$  and  $\partial_0^*$  are the forward and backward lattice derivatives, respectively, and  $c_A$  denotes the coefficient multiplying the  $O(a)$  improvement term in the improved axial current. It is understood that eq. (A.7) is evaluated for  $\theta = 0$ , whereas in all other cases the correlation functions have been computed for  $\theta = 1/2$ .

The lattice step scaling function  $\Sigma_P$  is then defined through

$$\Sigma_P(u, a/L) = \frac{Z_P(g_0, 2L/a)}{Z_P(g_0, L/a)} \quad \text{at } m(g_0) = 0, \quad \bar{g}^2(L) = u. \quad (\text{A.8})$$

Here,  $m(g_0)$  is always evaluated for lattice size  $L/a$  with  $x_0 = L/2$ . The condition  $m(g_0) = 0$  defines the critical value of the hopping parameter,  $\kappa_c$ , and the condition  $\bar{g}^2(L) = u$  specifies which value of the bare coupling  $g_0$  is to be used for a given value of  $L/a$ .

With these definitions the lattice step scaling function  $\Sigma_P$  is a function of the renormalized coupling  $u$ , up to cutoff effects. Its continuum limit is reached as  $a/L \rightarrow 0$  for fixed  $u$ .

### A.2.2 Details of the simulation

The correlation functions in eqs. (A.3), (A.4) and (A.6) have been evaluated in a lattice simulation using the  $O(a)$  improved Wilson action and the axial current defined in [31].

$L/a$	$c$	$L/a$	$c$
6	0.98969662	16	0.99853742
8	0.99417664	24	0.99934941
12	0.99740297	32	0.99963393

**Table 5:** Values for  $c$ , defined implicitly by  $Z_P(0, L/a) = 1$

In particular, the improvement coefficients  $c_{\text{sw}}$  and  $c_A$  given by eqs. (5.16) and (6.5) of that reference have been used.

As in the case of  $\Sigma$ , boundary  $\mathcal{O}(a)$  improvement terms have to be considered. In analogy to  $c_t$ , one also has to cancel the contributions of boundary terms arising from local composite operators involving quark fields. This is achieved by including a suitably chosen term in the action, whose coefficient is denoted by  $\tilde{c}_t$  [63]. Also  $\tilde{c}_t$  has only been determined in perturbation theory. We have used its perturbative expansion to one loop [73]

$$\tilde{c}_t^{1\text{-loop}} = 1 - 0.018g_0^2. \quad (\text{A.9})$$

The influence of the imperfectly known improvement coefficients  $c_t$  and  $\tilde{c}_t$  on the continuum extrapolation has to be investigated. In particular, it is not clear a priori whether an extrapolation of  $\Sigma_P$  in  $a^2/L^2$  is justified.

The constants  $Z_P(g_0, L/a)$  and  $Z_P(g_0, 2L/a)$  in eq. (A.8) have been evaluated for  $\theta = 1/2$  at the point where the current quark mass defined in eq. (A.7) vanishes. The point in  $\kappa$  where the condition  $m(g_0) = 0$  is satisfied is called the “critical” value of the hopping parameter,  $\kappa_c$ . In practice,  $\kappa_c$  has been obtained through an interpolation of the data for  $m(g_0)$  around the point where it vanishes.

We have evaluated  $\Sigma_P(u, a/L)$  at each of the 13 chosen values of  $u$  for  $L/a = 6, 8, 12$  and 16. The simulation algorithm is as specified before and the correlation functions were computed as detailed in Sect. 2 and Subsect. 3.2 of ref. [31]. “Measurements” of the correlation functions  $f_1$ ,  $f_A$  and  $f_P$  were separated by 5 full iterations of the algorithm on the smallest lattice, rising to 30 iterations on the largest. We have checked explicitly for the statistical independence of our sample by dividing the full ensemble into bins, each containing a number of individual “measurements”. The statistical errors were then monitored as the number of measurements per bin was increased. We did not observe any significant change of the errors in  $Z_P$  for increasing bin size, which we take as evidence for the statistical independence of all our samples.

Since boundary conditions  $C = C' = 0$  apply here, the correlation functions  $f_A$  and  $f_P$  could be averaged with their counterparts  $f'_A$  and  $f'_P$ , which are defined by a time-reflection applied to  $f_A$  and  $f_P$  (see eqs. (2.5) and (2.6) of ref. [31]).

The number of measurements was chosen such that the statistical error in  $Z_P(g_0, L/a)$  was typically a factor 2–3 smaller than that of  $Z_P(g_0, 2L/a)$ . Thereby it was ensured that the statistical error of  $\Sigma_P$  was dominated by the uncertainty in  $Z_P(g_0, 2L/a)$ . Typically, we have evaluated  $Z_P(g_0, L/a)$  on 200 – 640 configurations, whereas 60 – 120 measurements were accumulated for  $Z_P(g_0, 2L/a)$ .

Statistical errors were computed using the jackknife method. The error in  $\Sigma_P$  due to the uncertainty in the coupling was estimated using the one-loop expansion of  $\Sigma_P$  in  $u$ . It turned out to be about 10 times smaller than the statistical error in  $\Sigma_P$  in the whole range of  $u$  considered and has therefore been neglected in the error estimate. The error in  $\Sigma_P$  due to the uncertainty in  $\kappa_c$  has been estimated using the slopes for  $Z_P(g_0, L/a)$  and  $Z_P(g_0, 2L/a)$  computed for several values of the hopping parameter. It was found



that  $\Sigma_P$  depends rather weakly on the bare quark mass, so that the uncertainty in  $\Sigma_P$  from the error in  $\kappa_c$  was negligible.

Results for  $Z_P(g_0, L/a)$ ,  $Z_P(g_0, 2L/a)$ ,  $\kappa_c$  and the step scaling function  $\Sigma_P$  are shown in Table 6. The data in the last four rows were computed using the two-loop formula for  $c_t$  (see eq. (A.11) below).

### A.2.3 Continuum extrapolation of $\Sigma_P$

The next task is the extrapolation of  $\Sigma_P$  to the continuum limit for fixed coupling  $u$ . Our results for  $\Sigma_P$  show at most a weak dependence on the lattice spacing. Before performing an extrapolation we first investigate the question whether it is justified to assume that the leading cutoff effects are proportional to  $a^2/L^2$ , given that the improvement coefficients  $c_t$  and  $\tilde{c}_t$  are only known in perturbation theory.

We start by investigating the influence of  $\tilde{c}_t$  by comparing the step scaling function computed using the one-loop expression for  $\tilde{c}_t$  to the case where we artificially replace the one-loop coefficient by 10 times its value in eq. (A.9), viz.

$$\tilde{c}'_t = 1 - 0.180 g_0^2. \quad (\text{A.10})$$

For the range of bare couplings used in our simulations, this represents a change of up to 20%, which is surely a conservative estimate of the remainder of the perturbative series for  $\tilde{c}_t$ . We found that the change in  $\Sigma_P$  induced by replacing  $\tilde{c}_t^{1\text{-loop}}$  by  $\tilde{c}'_t$  amounts to around 0.8% for  $L/a = 6$  and  $u = 3.48$ , i.e. at the point where the effect is expected to be most pronounced. Furthermore, the difference in  $\Sigma_P$  decreases considerably for  $L/a = 8$  and/or smaller couplings. We conclude that the step scaling function is only weakly dependent on the value of  $\tilde{c}_t$ , and that the effect of using the one-loop estimate for  $\tilde{c}_t$  is negligible at the current level of precision.

To assess the influence of  $c_t$  on the cutoff dependence of  $\Sigma_P$ , one has to take into account that the bare coupling must be adjusted when  $c_t$  is changed in order to keep the renormalized coupling fixed. We have performed this analysis for fixed  $u = 3.48$  where the uncertainty in  $c_t$  is largest. We changed  $c_t$  by adding the two-loop term, which was only known towards the end of our numerical computations [65],

$$c_t^{2\text{-loop}} = 1 - 0.089 g_0^2 - 0.030 g_0^4. \quad (\text{A.11})$$

The corresponding change in  $\Sigma_P$  is  $\approx 1.5\%$  for  $L/a = 6$ , decreasing considerably as the resolution gets finer (cf. Table 6). We will show in the following that this  $O(a)$ -uncertainty, although statistically significant at non-zero  $a/L$ , does not affect our values for  $\sigma_P(u)$  obtained by continuum extrapolations.

$\beta$	$\kappa_c$	$L/a$	$\bar{g}^2(L)$	$Z_P(g_0, L/a)$	$Z_P(g_0, 2L/a)$	$\Sigma_P(u, a/L)$
10.7503	0.130591(4)	6	0.8873(5)	0.8476(5)	0.8187(13)	0.9659(17)
11.0000	0.130439(3)	8	0.8873(10)	0.8407(5)	0.8118(14)	0.9656(18)
11.3384	0.130251(2)	12	0.8873(30)	0.8314(6)	0.8035(10)	0.9664(14)
11.5736	0.130125(2)	16	0.8873(25)	0.8252(8)	0.7993(16)	0.9687(21)
10.0500	0.131073(5)	6	0.9944(7)	0.8334(5)	0.8010(13)	0.9612(17)
10.3000	0.130889(3)	8	0.9944(13)	0.8259(6)	0.7950(16)	0.9625(21)
10.6086	0.130692(2)	12	0.9944(30)	0.8143(7)	0.7868(13)	0.9662(18)
10.8910	0.130515(2)	16	0.9944(28)	0.8094(8)	0.7813(13)	0.9653(19)
9.5030	0.131514(5)	6	1.0989(8)	0.8190(6)	0.7822(13)	0.9551(18)
9.7500	0.131312(3)	8	1.0989(13)	0.8114(6)	0.7778(16)	0.9586(21)
10.0577	0.131079(3)	12	1.0989(40)	0.8007(7)	0.7688(12)	0.9602(17)
10.3419	0.130876(2)	16	1.0989(44)	0.7965(9)	0.7661(16)	0.9617(22)
8.8997	0.132072(9)	6	1.2430(13)	0.8015(6)	0.7638(16)	0.9529(21)
9.1544	0.131838(4)	8	1.2430(14)	0.7935(7)	0.7557(16)	0.9523(23)
9.5202	0.131503(3)	12	1.2430(35)	0.7853(7)	0.7498(14)	0.9548(20)
9.7350	0.131335(3)	16	1.2430(34)	0.7769(9)	0.7436(20)	0.9572(28)
8.6129	0.132380(6)	6	1.3293(12)	0.7917(6)	0.7489(17)	0.9460(22)
8.8500	0.132140(5)	8	1.3293(21)	0.7811(7)	0.7423(17)	0.9503(23)
9.1859	0.131814(3)	12	1.3293(60)	0.7736(8)	0.7344(15)	0.9494(22)
9.4381	0.131589(2)	16	1.3293(40)	0.7689(10)	0.7282(17)	0.9470(25)
8.3124	0.132734(10)	6	1.4300(20)	0.7808(8)	0.7347(19)	0.9410(26)
8.5598	0.132453(5)	8	1.4300(21)	0.7713(7)	0.7279(15)	0.9438(21)
8.9003	0.132095(3)	12	1.4300(50)	0.7627(8)	0.7195(18)	0.9434(25)
9.1415	0.131855(3)	16	1.4300(58)	0.7562(11)	0.7112(18)	0.9405(27)
7.9993	0.133118(7)	6	1.5553(15)	0.7663(7)	0.7181(20)	0.9371(28)
8.2500	0.132821(5)	8	1.5553(24)	0.7591(7)	0.7128(20)	0.9390(27)
8.5985	0.132427(3)	12	1.5533(70)	0.7483(9)	0.7046(14)	0.9415(22)
8.8323	0.132169(3)	16	1.5533(70)	0.7424(11)	0.6939(22)	0.9346(32)

**Table 6:** Results for the step scaling function  $\Sigma_P$

$\beta$	$\kappa_c$	$L/a$	$\bar{g}^2(L)$	$Z_P(g_0, L/a)$	$Z_P(g_0, 2L/a)$	$\Sigma_P(u, a/L)$
7.7170	0.133517(8)	6	1.6950(26)	0.7520(7)	0.7028(18)	0.9346(26)
7.9741	0.133179(5)	8	1.6950(28)	0.7454(8)	0.6972(19)	0.9354(28)
8.3218	0.132756(4)	12	1.6950(79)	0.7349(9)	0.6851(14)	0.9322(22)
8.5479	0.132485(3)	16	1.6950(90)	0.7281(11)	0.6779(20)	0.9312(31)
7.4082	0.133961(8)	6	1.8811(22)	0.7344(8)	0.6787(19)	0.9241(28)
7.6547	0.133632(6)	8	1.8811(28)	0.7268(8)	0.6693(22)	0.9209(32)
7.9993	0.133159(4)	12	1.8811(38)	0.7187(8)	0.6641(17)	0.9241(26)
8.2415	0.132847(3)	16	1.8811(99)	0.7104(11)	0.6588(20)	0.9274(32)
7.1214	0.134423(9)	6	2.1000(39)	0.7168(8)	0.6513(20)	0.9086(29)
7.3632	0.134088(6)	8	2.1000(45)	0.7073(8)	0.6472(21)	0.9151(31)
7.6985	0.133599(4)	12	2.1000(80)	0.6969(10)	0.6368(16)	0.9137(27)
7.9560	0.133229(3)	16	2.100(11)	0.6930(12)	0.6365(20)	0.9185(33)
6.7807	0.134994(11)	6	2.4484(37)	0.6874(10)	0.6117(21)	0.8899(32)
7.0197	0.134639(7)	8	2.4484(45)	0.6809(10)	0.6079(21)	0.8928(33)
7.3551	0.134141(5)	12	2.4484(80)	0.6685(10)	0.6004(18)	0.8981(30)
7.6101	0.133729(4)	16	2.448(17)	0.6688(12)	0.5956(20)	0.8905(34)
6.5512	0.135327(12)	6	2.770(7)	0.6629(11)	0.5799(18)	0.8747(30)
6.7860	0.135056(8)	8	2.770(7)	0.6572(10)	0.5731(21)	0.8720(35)
7.1190	0.134513(5)	12	2.770(11)	0.6496(10)	0.5667(18)	0.8724(31)
7.3686	0.134114(3)	16	2.770(14)	0.6448(11)	0.5671(23)	0.8795(39)
6.2204	0.135470(15)	6	3.480(8)	0.6181(12)	0.5063(20)	0.8190(36)
6.4527	0.135543(9)	8	3.480(14)	0.6114(10)	0.5061(32)	0.8277(54)
6.7750	0.135121(5)	12	3.480(39)	0.6089(11)	0.5076(24)	0.8336(42)
7.0203	0.134707(4)	16	3.480(21)	0.6063(12)	0.5114(26)	0.8434(47)
6.257	0.135499(14)	6	3.480(8)	0.6221(11)	0.5179(19)	0.8324(34)
6.476	0.135524(9)	8	3.480(8)	0.6166(10)	0.5143(23)	0.8341(40)
6.799	0.135090(6)	12	3.480(9)	0.6106(11)	0.5133(19)	0.8406(35)
7.026	0.134701(4)	16	3.480(13)	0.6070(13)	0.5137(27)	0.8464(48)

**Table 6:** (continued)

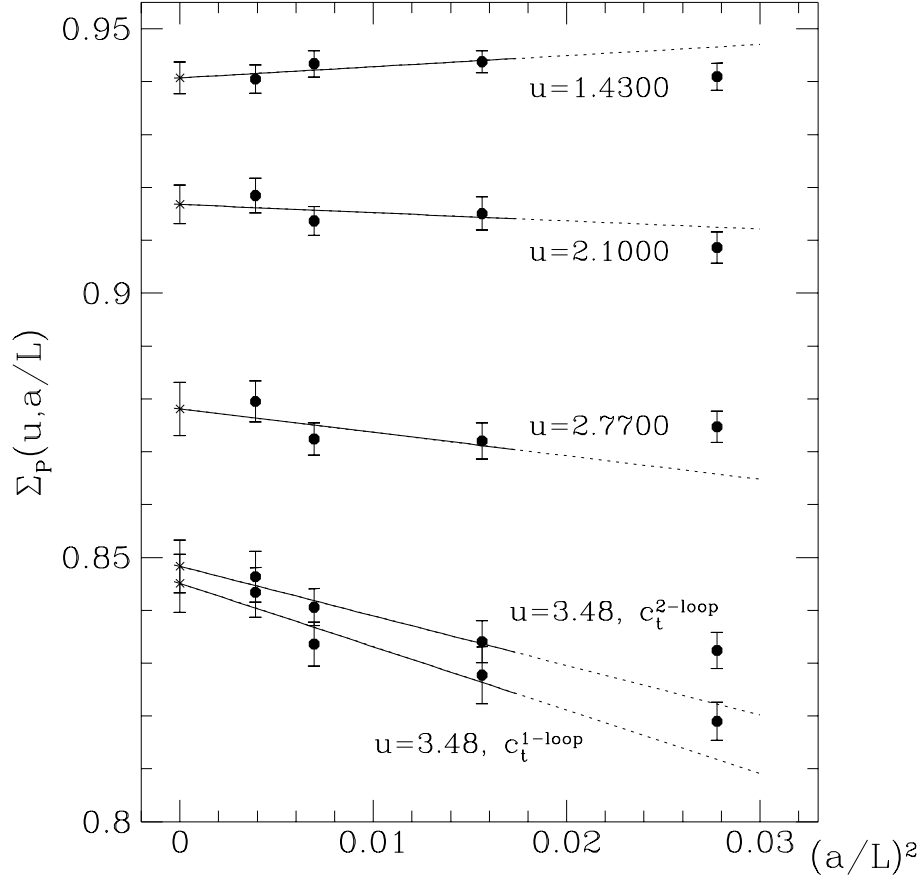


**Figure 8:** Examples of continuum extrapolations of  $\Sigma_P$  using Fit B. The dotted lines are the continuation of the fit functions to the data points for  $L/a = 6$ , which have been excluded from the fit.

The dependence of  $\Sigma_P$  on the lattice spacing is modelled using the following fit functions

$$\text{Fit A :} \quad \Sigma_P(u, a/L) = \sigma_P(u) + \rho(u) a/L \quad (\text{A.12})$$

$$\text{Fit B :} \quad \Sigma_P(u, a/L) = \sigma_P(u) + \rho'(u) a^2/L^2. \quad (\text{A.13})$$

In other words, we compare the approach to the continuum limit assuming that the leading cutoff effects are either linear (Fit A) or quadratic (Fit B) in  $a/L$ . Fit A is motivated by the fact that not all  $O(a)$  improvement terms are known non-perturbatively. As a safeguard against higher order cutoff effects, we exclude the data for  $\Sigma_P$  obtained on our coarsest lattices, i.e. for  $L/a = 6$  from the fits.

The extrapolated values for  $\sigma_P(u)$  show no significant dependence on the fit ansatz (Fit A or B) for all renormalized couplings  $u$ . The biggest effect is seen at the largest coupling, i.e.  $u = 3.48$ , where the results for  $\sigma_P(3.48)$  obtained from either Fit A or B

$u$	$\sigma_P(u)$	$\rho'(u)$	$\chi^2/n_{\text{df}}$
0.8873	0.9683(21)	-0.19(21)	0.51
0.9944	0.9672(23)	-0.28(23)	0.47
1.0989	0.9622(24)	-0.24(24)	0.09
1.2430	0.9579(29)	-0.36(28)	0.13
1.3293	0.9470(28)	0.23(28)	0.27
1.4300	0.9407(30)	0.21(27)	0.40
1.5553	0.9382(33)	0.11(33)	3.01
1.6950	0.9297(32)	0.36(33)	0.00
1.8811	0.9284(36)	-0.50(37)	0.21
2.1000	0.9168(37)	-0.16(37)	1.10
2.4484	0.8942(38)	-0.01(39)	3.04
2.7700	0.8781(42)	-0.44(41)	1.44
3.48	0.8451(55)	-1.20(59)	1.05
3.48*	0.8483(50)	-0.94(48)	0.26

**Table 7:** Continuum extrapolations of  $\Sigma_P$  using Fit B

differ by one standard deviation. Such an effect may be statistical or systematic. To test for the latter possibility, we consider the data for  $\Sigma_P(3.48, a/L)$  obtained using  $c_t = c_t^{2\text{-loop}}$ . Figure 8 demonstrates that cutoff effects of  $O(a)$  are reduced compared to  $c_t = c_t^{1\text{-loop}}$ . Furthermore, Fit B applied to the data set for  $c_t = c_t^{2\text{-loop}}$  produces an extrapolated value which is entirely consistent with the one obtained for  $c_t = c_t^{1\text{-loop}}$ . We conclude that the small uncertainties which are present in the improvement coefficients  $c_t, \tilde{c}_t$  are numerically unimportant, and that extrapolations using  $(a/L)^2$  terms as the dominant scaling violation are justified. We emphasize that such a statement can only be made for a given level of statistical accuracy. Furthermore we use only data for  $L/a = 8, 12$  and  $16$ , with the last point already fairly close to the continuum limit.

For our best estimates we have taken the results from Fit B, obtained for the standard one-loop result for  $c_t$ , and excluding the data for  $L/a = 6$ . Typical examples of extrapolations at selected values of  $u$  are shown in Fig. 8. The fit parameters for all extrapolations using Fit B are shown in Table 7, where the point computed using the two-loop expression for the improvement coefficient  $c_t$  is marked by an asterisk.

## B Error propagation in the scale evolution

In this appendix we provide further details about the numerical solution of the recursion relations (5.3) and (5.7), the principal aim being to explain how precisely the errors on the final results have been determined.

As discussed in Section 5, the calculation starts by fitting the data for the step

scaling functions listed in Table 1. In the case of the function  $\sigma(u)$  our fit ansatz is

$$\sigma(u) = u + \sigma_0 u^2 + \sigma_1 u^3 + \dots + \sigma_n u^{n+2}, \quad (\text{B.1})$$

where  $\sigma_2, \dots, \sigma_n$  are the fit parameters while

$$\sigma_0 = 2 \ln(2) b_0 \quad \text{and} \quad \sigma_1 = \sigma_0^2 + 2 \ln(2) b_1 \quad (\text{B.2})$$

are fixed to the values that one obtains in perturbation theory. The fit function for the other step scaling function is taken to be

$$\sigma_P(u) = 1 + \sigma_{P,0} u + \dots + \sigma_{P,n} u^{n+1}, \quad \sigma_{P,0} = -\ln(2) d_0. \quad (\text{B.3})$$

Least-squares fits with 1, 2 and 3 fit parameters have then been performed and were found to represent the data well (the curves shown in Figs. 3 and 5 are for 2 fit parameters).

The solution of the recursion relations (5.3) and (5.7) is unique once a definite expression for the step scaling functions is chosen. In particular, the calculated values of  $u_k$  and  $v_k$  are functions of the fit parameters. However, one should take into account that the data for the step scaling functions have errors and thus determine the fit parameters only within certain error margins. The errors on the step scaling functions are uncorrelated (they come from different simulation runs) and the errors on the fit parameters and the  $u_k$ 's and  $v_k$ 's are thus obtained straightforwardly by applying the usual rules for error propagation.

The question now arises to which extent the calculated values and error bounds are influenced by the choice of fit functions. We have made two independent checks to convince ourselves that this source of systematic error is under control. First we noted that compatible results with slightly larger errors are obtained if the number of fit parameters is increased. This is the expected behaviour, and since the fit quality is already good with one parameter, we decided to quote results for two fit parameters so as to be on the safe side.

The other check that we have made is to apply the fit procedure and error determination to simulated data sets that have been generated artificially, assuming  $\sigma(u)$  and  $\sigma_P(u)$  to be equal to some analytically given functions with roughly the right shape. Comparing with the “exact” solution of the recursion relations, we then found that the systematic bias arising from the choice of fit polynomials is not significant at the current level of precision.

## C Computation of $Z_P$ at the matching scale

Here we describe the details of the calculation of  $Z_P(g_0, L/a)_{L=1.436 r_0}$  required to connect the masses in the SF-scheme to the bare current quark masses. Our task is to compute  $Z_P$  for a range of bare couplings, which are commonly used in simulations in large physical volumes. In addition, we have to estimate the effect of using perturbation

$L/a$	$\beta = 6/g_0^2$	$c_t^{1\text{-loop}}$ $Z_P$	$c_t^{2\text{-loop}}$ $Z_P$
8	6.0219	0.5250(17)	0.5218(17)
10	6.1628	0.5211(17)	0.5177(19)
12	6.2885	0.5207(21)	0.5179(23)
16	6.4956	0.5160(17)	0.5157(19)

**Table 8:** Results for  $Z_P(g_0, L/a)$  at fixed scale  $L = 1.436 r_0$

theory for the improvement coefficients  $c_t$  and  $\tilde{c}_t$ , instead of non-perturbative values, which are currently not available. Since  $c_t$  is known to two loops, we have computed  $Z_P$  using both the one- and two-loop expressions, in order to assess the influence on the final estimates.

Our procedure is as follows. First we choose pairs of  $(\beta, L/a)$  such that  $L/a = 1.436 r_0/a$ , using lattice data for  $r_0/a$  from [67]. For a chosen value of  $L/a$  this condition determines the corresponding  $\beta$ -value, which is obtained by inserting  $a/r_0 = 1.436(a/L)$  into the parametrization of  $\ln(a/r_0)$  quoted in eq. (2.18) of ref. [67], viz.

$$\ln(a/r_0) = -1.6805 - 1.7139(\beta - 6) + 0.8155(\beta - 6)^2 - 0.6667(\beta - 6)^3. \quad (\text{C.1})$$

Solving numerically for  $\beta$  yields the desired combination of  $(\beta, L/a)$ .  $Z_P$  is then computed for  $\theta = 0.5$  using the normalization condition eq. (A.5) at the critical value of the hopping parameter determined for lattice size  $L/a$ .

This procedure yields  $\beta$  with finite accuracy, and the error which propagates into  $Z_P$  can be estimated using one-loop perturbation theory. This error can be neglected, since it is more than 10 times smaller than the statistical error in  $Z_P$ . Results for  $Z_P(g_0, L/a)_{L=1.436 r_0}$  computed using both the one- and two-loop expressions for  $c_t$  are listed in Table 8.

In principle one could compute  $Z_P$  for smaller values of  $\beta$  and  $L/a$ . However, for  $L/a = 6$  the condition  $L = 1.436 r_0$  implies  $\beta < 6.0$ , where the parametrizations of  $c_{\text{sw}}$  and  $c_A$  from ref. [31] cannot be used. In order to have an additional value at  $\beta = 6.0$ , we have applied a special procedure. We have computed  $Z_P$  for  $\beta = 6.0$  fixed, but using different lattice sizes for which  $L/r_0$  straddles the reference value  $L/r_0 = 1.436$ . An interpolation in  $L/r_0$  at fixed  $\beta$  then yields the desired result for  $Z_P(g_0 = 1, L/a)_{L=1.436 r_0}$ .

Using the parametrization of  $r_0/a$ , eq. (2.18) in [67] we find

$$r_0/a = 5.368(22), \quad \beta = 6.0, \quad (\text{C.2})$$

and the results for  $Z_P$  for three different values of  $L/r_0$  are listed in Table 9.

$L/a$	$L/r_0$	$c_t^{1\text{-loop}}$ $Z_P(g_0 = 1, L/a)$	$c_t^{2\text{-loop}}$ $Z_P(g_0 = 1, L/a)$
6	1.1177(46)	0.5728(26)	0.5712(27)
8	1.4903(61)	0.5197(24)	0.5171(26)
10	1.8629(76)	0.4590(31)	0.4584(30)

**Table 9:** Values of  $Z_P$  at  $\beta = 6.0$  for  $L$  around  $L = 1.436 r_0$

A quadratic interpolation in  $L/r_0$  of the data in the table yields

$$Z_P(g_0 = 1, L/a)_{L=1.436 r_0} = \begin{cases} 0.5279(24), & c_t^{1\text{-loop}} \\ 0.5253(26), & c_t^{2\text{-loop}} \end{cases} . \quad (\text{C.3})$$

The results for  $Z_P(g_0, L/a)_{L=1.436 r_0}$  for  $6.0 \leq \beta \leq 6.5$ , using either  $c_t^{1\text{-loop}}$  or  $c_t^{2\text{-loop}}$  can be parametrized by a polynomial fit in  $(\beta - 6)$ . For  $c_t^{2\text{-loop}}$  the result is shown in eq. (6.9).

We end this appendix with a brief comment on the influence of  $\tilde{c}_t$  on the estimates of  $Z_P$ . Similarly to the case of  $\Sigma_P$ , this has been investigated by repeating the computation of  $Z_P$  at  $\beta = 6.0$  using  $\tilde{c}_t$  with its one-loop coefficient multiplied by a factor 10. It turned out that the resulting interpolated value of  $Z_P(1, L/a)_{L=1.436 r_0}$  did not change appreciably within statistical errors. We conclude that the influence of  $\tilde{c}_t$  can be neglected at the present level of precision.

## References

- [1] H. Leutwyler, Phys. Lett. B378 (1996) 313, hep-ph/9602366.
- [2] C.R. Allton, M. Ciuchini, M. Crisafulli, E. Franco, V. Lubicz and G. Martinelli, Nucl. Phys. B431 (1994) 667, hep-ph/9406263.
- [3] C.R. Allton, V. Giménez, L. Giusti and F. Rapuano, Nucl. Phys. B489 (1997) 427, hep-lat/9611021.
- [4] V. Giménez, L. Giusti, F. Rapuano and M. Talevi, (1998), hep-lat/9801028; L. Giusti, V. Giménez, F. Rapuano, M. Talevi and A. Vladikas, (1998), hep-lat/9809037.
- [5] UKQCD Collaboration, C.R. Allton et al., Phys. Rev. D49 (1994) 474, hep-lat/9309002.
- [6] R. Gupta and T. Bhattacharya, Phys. Rev. D55 (1997) 7203, hep-lat/9605039.



- [7] B.J. Gough, G.M. Hockney, A.X. El-Khadra, A.S. Kronfeld, P.B. Mackenzie, B.P. Mertens, T. Onogi and J.N. Simone, Phys. Rev. Lett. 79 (1997) 1622, hep-ph/9610223.
- [8] M. Göckeler, R. Horsley, H. Perlt, P. Rakow, G. Schierholz, A. Schiller and P. Stephenson, Phys. Rev. D57 (1997) 5562, hep-lat/9707021.
- [9] M. Göckeler et al., (1998), hep-lat/9810006.
- [10] CP-PACS Collaboration, S. Aoki et al., Nucl. Phys. B (Proc. Suppl.) 63 (1998) 161, hep-lat/9709139; CP-PACS Collaboration, K. Kanaya et al., (1998), hep-lat/9809120 and hep-lat/9809146.
- [11] A. Cucchieri, M. Masetti, T. Mendes and R. Petronzio, Phys. Lett. B422 (1998) 212, hep-lat/9711040; A. Cucchieri, T. Mendes and R. Petronzio, J. High Energy Phys. 05 (1998) 006, hep-lat/9804007.
- [12] D. Becirevic, Ph. Boucaud, J.P. Leroy, V. Lubicz, G. Martinelli and F. Mescia, (1998), hep-lat/9807046; D. Becirevic, Ph. Boucaud, L. Giusti, J.P. Leroy, V. Lubicz, G. Martinelli and F. Mescia, (1998), hep-lat/9809187.
- [13] SESAM Collaboration, N. Eicker et al., Phys. Lett. B407 (1997) 290, hep-lat/9704019; SESAM Collaboration, N. Eicker et al., (1998), hep-lat/9806027.
- [14] J. Bijnens, J. Prades and E. de Rafael, Phys. Lett. B348 (1995) 226, hep-ph/9411285.
- [15] M. Jamin and M. Münz, Z. Phys. C66 (1995) 633, hep-ph/9409335.
- [16] M. Jamin, Nucl. Phys. (Proc. Suppl.) 64 (1998) 250, hep-ph/9709484.
- [17] S. Narison, Phys. Lett. B358 (1995) 113, hep-ph/9504333.
- [18] K.G. Chetyrkin, D. Pirjol and K. Schilcher, Phys. Lett. B404 (1997) 337, hep-ph/9612394.
- [19] P. Colangelo, F.D. Fazio, G. Nardulli and N. Paver, Phys. Lett. B408 (1997) 340, hep-ph/9704249.
- [20] J. Prades, Nucl. Phys. (Proc. Suppl.) 64 (1998) 253, hep-ph/9708395.
- [21] F.J. Ynduráin, Nucl. Phys. B517 (1998) 324, hep-ph/9708300.
- [22] H.G. Dosch and S. Narison, Phys. Lett. B417 (1998) 173, hep-ph/9709215.
- [23] L. Lellouch, E. de Rafael and J. Taron, Phys. Lett. B414 (1997) 195, hep-ph/9707523.

- [24] T. Bhattacharya and R. Gupta, Nucl. Phys. B (Proc. Suppl.) 63 (1998) 95, hep-lat/9710095.
- [25] R. Gupta, Introduction to Lattice QCD, Lectures given at Les Houches Summer School in Theoretical Physics, Probing the Standard Model of Particle Interactions, Les Houches, France, 28 Jul – 5 Sep 1997, hep-lat/9807028.
- [26] K. Jansen, C. Liu, M. Lüscher, H. Simma, S. Sint, R. Sommer, P. Weisz and U. Wolff, Phys. Lett. B372 (1996) 275, hep-lat/9512009.
- [27] M. Lüscher, Advanced Lattice QCD, Lectures given at Les Houches Summer School in Theoretical Physics, Probing the Standard Model of Particle Interactions, Les Houches, France, 28 Jul – 5 Sep 1997, hep-lat/9802029.
- [28] G. Martinelli, C. Pittori, C.T. Sachrajda, M. Testa and A. Vladikas, Nucl. Phys. B445 (1995) 81, hep-lat/9411010.
- [29] M. Göckeler, R. Horsley, H. Oelrich, H. Perlt, D. Petters, P.E.L. Rakow, A. Schäfer, G. Schierholz and A. Schiller, (1998), hep-lat/9809001.
- [30] V. Giménez, L. Giusti, F. Rapuano and M. Talevi, (1998), hep-lat/9806006.
- [31] M. Lüscher, S. Sint, R. Sommer, P. Weisz and U. Wolff, Nucl. Phys. B491 (1997) 323, hep-lat/9609035.
- [32] M. Lüscher, R. Sommer, P. Weisz and U. Wolff, Nucl. Phys. B413 (1994) 481, hep-lat/9309005.
- [33] S. Capitani, M. Guagnelli, M. Lüscher, S. Sint, R. Sommer, P. Weisz and H. Wittig, Nucl. Phys. B (Proc. Suppl.) 63 (1998) 153, hep-lat/9709125.
- [34] G. 't Hooft, Nucl. Phys. B61 (1973) 455.
- [35] W.A. Bardeen, A.J. Buras, D.W. Duke and T. Muta, Phys. Rev. D18 (1978) 3998.
- [36] ALPHA Collaboration, S. Sint and P. Weisz, (1998), hep-lat/9808013.
- [37] J. Gasser and H. Leutwyler, Phys. Rept. 87 (1982) 77; Ann. Phys. 158 (1984) 142; Nucl. Phys. B250 (1985) 465.
- [38] W.E. Caswell, Phys. Rev. Lett. 33 (1974) 244.
- [39] D.R.T. Jones, Nucl. Phys. B75 (1974) 531.
- [40] R. Tarrach, Nucl. Phys. B183 (1981) 384.
- [41] O. Nachtmann and W. Wetzel, Nucl. Phys. B187 (1981) 333.
- [42] O.V. Tarasov, A.A. Vladimirov and A.Y. Zharkov, Phys. Lett. 93B (1980) 429.

- [43] O.V. Tarasov, preprint JINR-P2-82-900 (1982), unpublished.
- [44] S.A. Larin and J.A.M. Vermaseren, Phys. Lett. B303 (1993) 334, hep-ph/9302208.
- [45] S.A. Larin, in: Proc. Int. Baksan School, “Particles and cosmology”, p. 216.
- [46] T. van Ritbergen, J.A.M. Vermaseren and S.A. Larin, Phys. Lett. B400 (1997) 379, hep-ph/9701390.
- [47] K.G. Chetyrkin, Phys. Lett. B404 (1997) 161, hep-ph/9703278.
- [48] J.A.M. Vermaseren, S.A. Larin and T. van Ritbergen, Phys. Lett. B405 (1997) 327, hep-ph/9703284.
- [49] M. Lüscher, R. Narayanan, P. Weisz and U. Wolff, Nucl. Phys. B384 (1992) 168, hep-lat/9207009.
- [50] S. Sint, Nucl. Phys. B421 (1994) 135, hep-lat/9312079.
- [51] S. Sint, Nucl. Phys. B451 (1995) 416, hep-lat/9504005.
- [52] S. Sint and R. Sommer, Nucl. Phys. B465 (1996) 71, hep-lat/9508012.
- [53] M. Lüscher, P. Weisz and U. Wolff, Nucl. Phys. B359 (1991) 221.
- [54] M. Bochicchio, L. Maiani, G. Martinelli, G.C. Rossi and M. Testa, Nucl. Phys. B262 (1985) 331.
- [55] L. Maiani and G. Martinelli, Phys. Lett. 178B (1986) 265.
- [56] G. Heatlie, G. Martinelli, C. Pittori, G.C. Rossi and C.T. Sachrajda, Nucl. Phys. B352 (1991) 266.
- [57] G. Martinelli, C.T. Sachrajda and A. Vladikas, Nucl. Phys. B358 (1991) 212.
- [58] G. Martinelli, C.T. Sachrajda, G. Salina and A. Vladikas, Nucl. Phys. B378 (1992) 591.
- [59] G. Martinelli, S. Petrarca, C.T. Sachrajda and A. Vladikas, Phys. Lett. B311 (1993) 241.
- [60] M.L. Paciello, S. Petrarca, B. Taglienti and A. Vladikas, Phys. Lett. B341 (1994) 187, hep-lat/9409012.
- [61] UKQCD Collaboration, D.S. Henty et al., Phys. Rev. D51 (1995) 5323, hep-lat/9412088.
- [62] M. Lüscher, S. Sint, R. Sommer and H. Wittig, Nucl. Phys. B491 (1997) 344, hep-lat/9611015.

- [63] M. Lüscher, S. Sint, R. Sommer and P. Weisz, Nucl. Phys. B478 (1996) 365, hep-lat/9605038.
- [64] M. Lüscher and P. Weisz, Commun. Math. Phys. 97 (1985) 59.
- [65] A. Bode, Nucl. Phys. B (Proc. Suppl.) 63 (1998) 796, hep-lat/9710043; A. Bode, P. Weisz and U. Wolff, (1998), hep-lat/9809175.
- [66] R. Sommer, Nucl. Phys. B411 (1994) 839, hep-lat/9310022.
- [67] ALPHA Collaboration, M. Guagnelli, R. Sommer and H. Wittig, (1998), hep-lat/9806005.
- [68] T. Bhattacharya, S. Chandrasekharan, R. Gupta, W. Lee and S. Sharpe, (1998), hep-lat/9810018.
- [69] S. Sint and P. Weisz, Nucl. Phys. B502 (1997) 251, hep-lat/9704001.
- [70] G.M. de Divitiis and R. Petronzio, Phys. Lett. B419 (1998) 311, hep-lat/9710071.
- [71] M. Guagnelli, J. Heitger, R. Sommer and H. Wittig, in preparation.
- [72] M. Guagnelli, K. Jansen and R. Petronzio, (1998), hep-lat/9809009.
- [73] M. Lüscher and P. Weisz, Nucl. Phys. B479 (1996) 429, hep-lat/9606016.